Chinese Chemical Letters 34 (2023) 107674

Contents lists available at ScienceDirect

Chinese Chemical Letters

journal homepage: www.elsevier.com/locate/cclet

Coumarin-based two-photon AIE fluorophores: Photophysical properties and biological application

Yitong Yang[a], Hao Zhong[a], Benhua Wang[a], Xiaojie Ren[b,*], Xiangzhi Song[a,*]

[a] College of Chemistry and Chemical Engineering, Central South University, Changsha 410083, China
[b] Department of Chemistry and Center of Super-Diamond and Advanced Films (COSDAF), City University of Hong Kong, Hong Kong 999077, China

ARTICLE INFO

Article history:
Received 14 March 2022
Revised 8 July 2022
Accepted 11 July 2022
Available online 12 July 2022

Keywords:
Fluorescent dyes
AIE
Two-photon
Large Stokes shifts
Lipid droplets

ABSTRACT

Based on the coumarin skeleton, we deliberately designed two groups of fluorophores, termed as Coum-R and Naph-Coum-R, using the diphenylamino group as the electron donor, which displayed long-wavelength emissions (red spectral region), large Stokes shift (up to 204 nm), superior AIE performance, and large two-photon absorbance cross-sections (as high as 365 GM). The electron-withdrawing substituents at the 3-position of these dyes could induce a significant red-shift in their emission spectra. Preliminary imaging experiments demonstrated the capability of these dyes as two-photon fluorophores for specifically staining lipid droplets in living cells.

Fluorescence has become an indispensable tool for visualizing the localization and dynamics of cellular organelles because of its high sensitivity, good selectivity, excellent spatial resolution, and non-invasiveness [1]. Generally, most fluorophores are weakly fluorescence in the aggregate state or solid state due to the aggregation-caused quenching (ACQ) effect [2,3]. In recent years, AIE fluorophores have emerged as a solution to the aggregation-caused self-quenching of fluorophores and are strongly fluorescent in the aggregated state [4].

Coumarin fluorophores are widely used in fluorescence detection because of their good photophysical properties [5], biocompatibility, and easy structural modification [6–8]. By replacing the diethylamino electron donor with diphenylamino group in 7-diethylaminocoumarin, Jiang's group obtained a new dye, DPACP, which shows excellent AIE characteristics [9]. However, DPACP emits in the short-wavelength spectral region (λ_{max} = 464 nm in toluene), which suffers from undesirable background interference in fluorescence sensing [9]. So far, coumarin fluorophores having diphenylamino donors are rarely reported [10,11]. In coumarin fluorophores, the electron-donating group at 4-positon produce a significant blue-shift in the optical spectra, whereas electron-withdrawing substituents at 3-positon induce a large red-shift [12]. Thus, we envisaged that it would be very interesting to develop more 7-diphenylaminocoumarin fluorophores with different substituents and study the substitution effect on their photophysical properties.

Compared with one-photon fluorophores, two-photon (TP) ones double the excitation wavelength offering deeper tissue penetration, lower background interference, and less photodamage to biological organisms [13–15]. Donor-acceptor fluorophores with diphenylamino electron donor usually display TP properties [16–18]. Unfortunately, it was not determined whether DPACP displayed TP properties or not. In addition, most D-A fluorophores having naphthalene platforms exhibit TP properties, and the enlarged conjugated system of naphthalene moiety can also red-shift the optical wavelengths [19,20]. Therefore, several naphthalene-based coumarin fluorophores have been developed as TP sensing probes [20–22]. However, the rigid and planar structure of the naphthalene moiety is prone to the ACQ effect [23,24]. Hence, it is necessary to modify the structure of naphthalene-based fluorophores to endow them with TP excitation, AIE property, and long-wavelength emission.

In this work, we first prepared diphenylaminocoumarins with different electron-withdrawing substituents at 3-position, named Coum-R, and investigated their photophysical properties to determine whether they show TP properties and to study the substituent effect (Scheme 1). Further, we replaced the benzene ring with naphthalene to obtain diphenylaminobenzo[*g*]coumarins, named Naph-Coum-R, and expected to have a longer optical wavelength. Gratifyingly, both Coum-R and Naph-Coum-R dyes displayed long-wavelength emission, large Stokes shift, two-photon properties, superior AIE performance, and red fluorescence in solid

* Corresponding authors.
E-mail addresses: renjie_8012@163.com (X. Ren), xzsong@csu.edu.cn (X. Song).

https://doi.org/10.1016/j.cclet.2022.07.017
1001-8417/

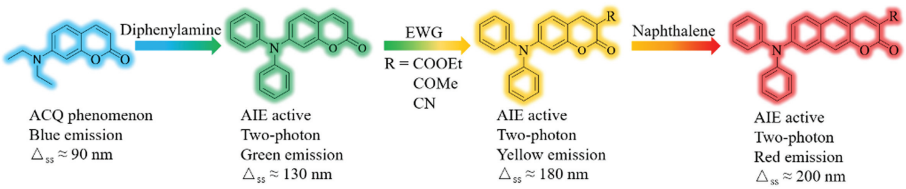

Scheme 1. Design strategy and molecular structures of coumarin-based fluorophores.

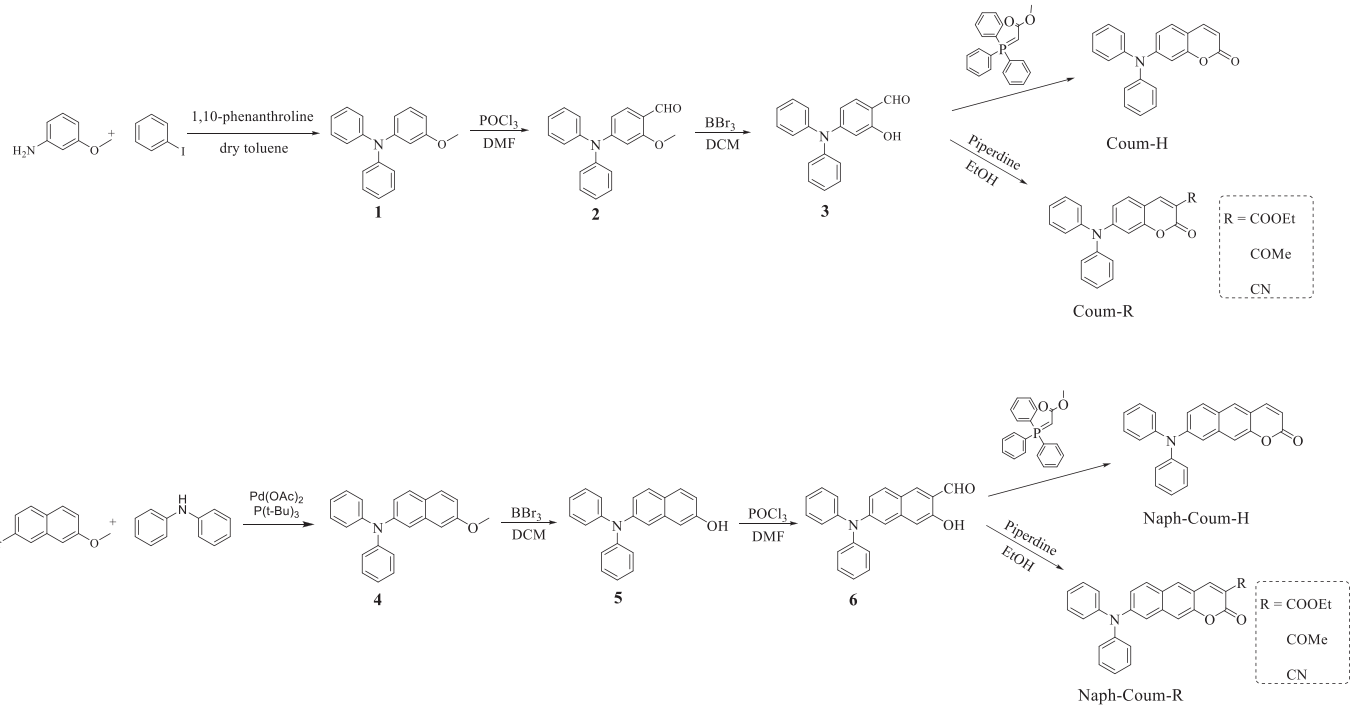

Scheme 2. Synthetic routes of Coum-R and Naph-Coum-R fluorophores.

state. These two-photon fluorophores displayed specific targeting ability towards lipid droplets in cells.

The synthesis of Coum-R and Naph-Coum-R dyes is illustrated in Scheme 2. Coum-R dyes were synthesized according to the reported methods [25,26]. Naph-Coum-R dyes were prepared in four steps using compound **4** as the starting material. Naph-Coum-COOEt, Naph-Coum-COMe, and Naph-Coum-CN were prepared by condensing compound **6** with active methylene compounds (ethyl-acetoacetate, diethyl propanedioate and ethyl cyanoacetate, respectively) through Knoevenagel reaction and a subsequent intramolecular nucleophilic substitution reaction. To synthesized Naph-Coum-H, methyl (triphenylphosphoranylidene)acetate was reacted with compound **6**. All these compounds were fully characterized by ^{1}H NMR, ^{13}C NMR and HRMS analysis. The detailed experiments and corresponding characterization date are presented in the Supporting information.

The photophysical properties of Coum-R and Naph-Coum-R dyes in different solvents were investigated, and the results are summarized in Table 1. It is evident that introducing electron-withdrawing groups at 3-position in Coum-R and Naph-Coum-R dyes resulted in a large red-shift in their absorption and emission spectra, and the extent of the red-shift is in the same order of the strength of the electron-withdrawing ability of the substituents. In addition, the Stokes shift also increased due to the presence of the electron-withdrawing substituents at 3-position. For example, the absorption maxima of Naph-Coum-H, Naph-Coum-COOEt, Naph-Coum-COMe and Naph-Coum-COCN in dichloromethane were 404, 452, 470, and 480 nm, and their emission maxima were 538, 642, 674, and 678 nm, respectively (Table 1 and Fig. 1). These results imply that the intramolecular charge transfer (ICT) effect enhanced in the order of Naph-Coum-H < Naph-Coum-COOEt < Naph-Coum-COMe < Naph-Coum-CN, consistent with the order of the electron-withdrawing ability of the substituents (H < COOEt < COMe < CN) [27]. With the increasing polarity of the solvents, the emission maxima were enlengthened, and the Stokes shifts also enlarged (Table 1 and Fig. 2). Exceptionally, the absorption maxima of Coum-R dyes in dioxane are shorter than that in toluene and dichloromethane. Compared with Coum-R dyes, the corresponding Naph-Coum-R dyes exhibited 20–47 nm red-shift in their absorption spectra, while their emission spectra were red-shifted by 18–78 nm due to the expanded conjugation system from the naphthalene moiety [28]. For example, the absorption maxima

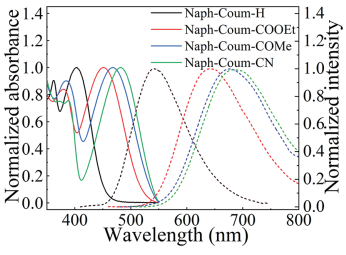

Fig. 1. Normalized absorption (solid line) and emission (dotted line) spectra of Naph-Coum-R dyes in dichloromethane.

Table 1
Photophysical properties of Naph-Coum-R and Coum-R dyes in various solvents.

-R	Solvent	Coum-R				Naph-Coum-R					
		$\lambda_{abs}/\lambda_{em}$(nm)	$\triangle_{ss}$ (nm)	Φ_f[a]	τ (ns)	ε_{max}[b] ($\times 10^4$)	$\lambda_{abs}/\lambda_{em}$ (nm)	$\triangle_{ss}$ (nm)	Φ_f[a]	τ (ns)	ε_{max}[b] ($\times 10^4$)
-H	Toluene	378/459	81	0.86	4.96	2.98	397/477	80	0.85	4.94	1.14
	1,4-Dioxane	376/472	96	0.96	5.79	2.99	394/489	95	0.33	5.77	1.39
	DCM	381/510	129	0.68	6.24	2.89	404/538	134	0.66	6.51	1.17
	Solid state	410/523	113	–	–	–	440/550	110	–	–	–
-COOEt	Toluene	413/515	102	0.74	5.24	3.62	439/571	132	0.65	8.22	1.01
	1,4-Dioxane	409/536	127	0.33	5.58	4.40	431/587	156	0.24	9.74	1.03
	DCM	417/596	179	0.12	1.94	2.87	452/642	190	0.13	3.96	1.01
	Solid state	430/535	105	–	–	–	454/625	171	–	–	–
-COMe	Toluene	427/532	105	0.74	5.21	3.23	453/597	144	0.67	7.31	1.08
	1,4-Dioxane	423/553	130	0.35	5.48	3.54	450 /616	166	0.24	7.38	1.08
	DCM	430/611	181	0.08	1.06	2.83	470/674	204	0.09	1.91	1.02
	Solid state	430/539	109	–	–	–	440/624	184	–	–	–
-CN	Toluene	429/538	109	0.75	5.82	3.27	461/616	155	0.73	5.97	0.82
	1,4-Dioxane	411/570	159	0.16	5.25	4.07	456/640	184	0.16	5.29	0.86
	DCM	433/620	187	0.04	0.74	2.93	480/678	198	0.14	1.19	0.74
	Solid state	459/580	121	–	–	–	450/625	175	–	–	–

[a] The relative fluorescence quantum yield for Coum-R and Naph-Coum-R using coumarin 7 ($\Phi_f = 0.82$ in MeOH) and coumarin 102 ($\Phi_f = 0.79$ in MeOH) as a reference, respectively.
[b] Molar absorptivity (L mol^{-1} cm^{-1}). "-" Represents untested data.

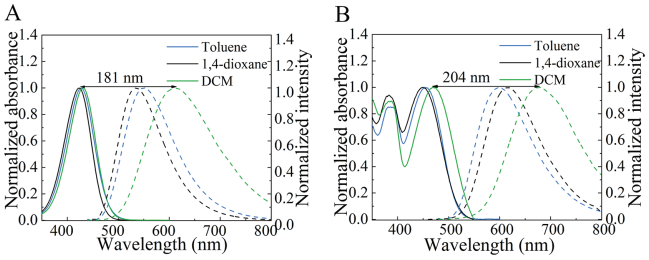

Fig. 2. Normalized absorption (solid line) and emission (dotted line) spectra of dyes Coum-COMe (A) and Naph-Coum-COMe (B) in different solvents.

of Coum-COMe and Naph-Coum-COMe in DCM were 430 nm and 470 nm, and their emission spectra peaked at 611 nm and 674 nm, respectively (Fig. 2). Different from Coum-R dyes, Naph-Coum-R dyes showed two broad absorption peaks, indicating that naphthalene moiety has two dipole moments with different vectors and their molar absorptivities were smaller (Fig. S1 in Supporting information) [29].

We were delighted that all Coum-R and Naph-Coum-R dyes exhibited quite large Stokes shifts (up to 204 nm), which could avoid the self-absorption and the interference between excitation and emission signals during fluorescence sensing. Noteworthy, Coum-R and Naph-Coum-R dyes with electron withdrawing groups -COOEt, COMe, and CN, displayed higher sensitivity to solvent polarity. For instance, in Coum-COMe the emission wavelength extended from 532 nm to 611 nm when changing the solvent from toluene to chloromethane (Fig. 2A), attributed to the enhanced ICT effect with increasing the polarity of the solvent [18].

To gain better insight into the optical properties, density functional theory (DFT) calculations were performed on Coum-R and Naph-Coum-R dyes using the Gaussian 09 program. The spatial distributions and frontier energy levels (HOMO & LUMO) were explored using DFT/B3LYP(6-311G). As show in Fig. S6 (Supporting information), the π electron cloud density of HOMO orbital is mainly distributed on the diphenylamino group and naphthalene moiety, whereas the π electron cloud density of LUMO orbital is focused on the coumarin core, showing an ICT effect upon excitation. Moreover, the introduction of electron-withdrawing substituents at the 3-position of Coum-R and Naph-Coum-R dyes intensified the ICT effect. As a result, the 3.20 eV energy gap between HOMO and LUMO of Naph-Coum-H decreased to 2.86 eV in Naph-Coum-CN, which well consistent with the absorption spectral results. Thus, compared to Coum-R dyes, the extended conjugated structure of Naph-Coum-R reduced the HOMO-LUMO energy gap, causing the absorption spectrum red-shift.

Since fluorescent quantum yield (Φ) and lifetimes (τ) are important parameters for fluorophores, we then determined Φ and τ of all the investigated dyes (Table 1). The values of fluorescent quantum yields and lifetimes were high for all the dyes in toluene, the Φ were 0.85, 0.65, 0.67, and 0.73 for Naph-Coum-H, Naph-Coum-COOEt, Naph-Coum-COMe and Naph-Coum-CN, respectively. In contrast, Φ of all the dyes significantly dropped when changing the solvent from nonpolar toluene to polar dioxane and dichloromethane, *e.g.*, Φ of Naph-Coum-COOEt dropped from 0.65 in toluene to 0.13 in dichloromethane and τ dropped from 8.22 in toluene to 3.96 in dichloromethane. The effect of solvent polarity on Φ can be attributed to the formation of a twisted intramolecular charge transfer state (TICT) [30]. In the excited state in polar solvents, the diphenylamino group of the investigated dye molecules could twist to form the TICT state to dissipate the energy, thereby increasing the non-radiative decay rate and caused the decrease of Φ and τ values. Moreover, the photostability of Coum-R and Naph-Coum-R were assessed in dioxane under a 500 W Xe lamp. As shown in Fig. S5 (Supporting information), all the dyes showed a good photostability.

All Coum-R and Naph-Coum-R dyes exhibited bright fluorescence in the solid state, as observed in Table 1 and Figs. 3 and 4. In the solid state, the twisted three-dimensional structure of the diphenylamino group could effectively prevent the intramolecular π-π stacking, and the rotation of two phenyl rings in the diphenylamino group was also inhibited. As a result, the non-radiative processes in the excited state of Coum-R and Naph-Coum-R dyes were largely inhibited [31]. Coum-H, Coum-COMe, and Coum-COOEt exhibited green fluorescence in the solid state, and Coum-CN had yellow fluorescence, which was attributed to the enhanced ICT effect of the electron-withdrawing substituents at 3-position. For Naph-Coum-R dyes, the naphthalene moiety greatly extended the conjugation system, which pushed their emission into the long-wavelength spectral region as compared to the Coum-R dyes. Consequently, all Naph-Coum-R dyes except Naph-Coum-H displayed red fluorescence in the solid state.

We next studied the AIE properties of Coum-R and Naph-Coum-R dyes in the mixture of DMSO-H_2O with different water fractions (f_w). As shown in Fig. 5, Coum-COOEt was very weakly fluorescent when the f_w was below 70%. Strong fluorescence was observed

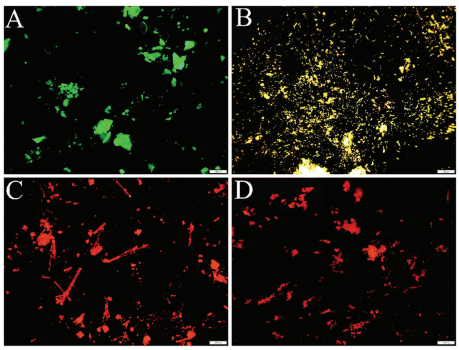

Fig. 3. Fluorescence images of Coum-COMe (A) Coum-CN (B) Naph-Coum-COMe (C), and Naph-Coum-CN (D) in solid state under 10 × fluorescence inverse microscope. Scale bar: 100 μm.

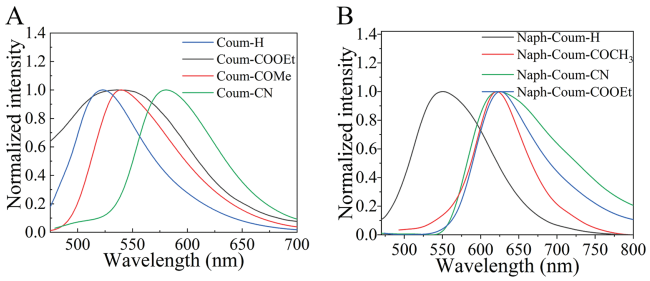

Fig. 4. Normalized emission spectra of Coum-R (A) and Naph-Coum-R (B) dyes in the solid state.

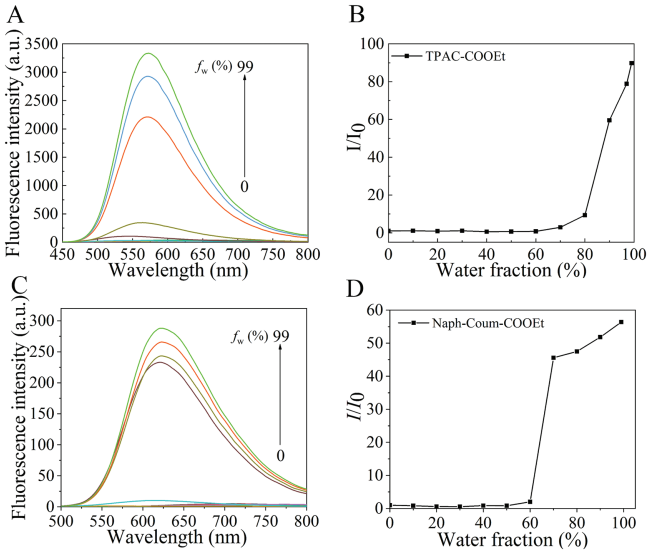

Fig. 5. Fluorescence spectra (left column) and fluorescence enhancement (I/I_0) (right column) of Coum-COOEt (A and B) and Naph-Coum-COOEt (C and D) in DMSO-H_2O mixture at different f_w when excited at 400 nm.

above 90% f_w and the fluorescence enhanced 85-fold when the f_w went from 0% to 99%. Naph-Coum-COOEt also showed strong red fluorescence over 70% f_w. The remaining dyes also showed superior AIE performance (Fig. S3 in Supporing information). However, the fluorescence of Naph-Coum-H, Naph-Coum-COMe and Naph-Coum-CN decreased rapidly at $f_w = 99\%$, because of the sample sedimentation. These results demonstrated that Coum-R and Naph-Coum-R dyes were good AIE fluorophores. To better understand their AIE properties, DFT and TD-DFT calculations were performed on Naph-Coum-COOEt, and the results are presented in Fig. S7 (Supporting information). In the ground state, the optimized dihedral angle between diphenylamino moiety and naphthalene core was 33°, which significantly twisted to 64° upon excitation, increasing the non-radiative decay rate. However, the intramolecular twist motion gets restricted in the aggregate state, making the dye strongly fluorescent [32].

Previous studies have shown that chromophores containing triphenylamine donor(s) or naphthalene moiety exhibit two-photon (TP) absorption properties [18,33]. Therefore, we decided to investigate the TP properties of Coum-R and Naph-Coum-R dyes using rhodamine B in methanol as a reference. As displayed in Fig. 6, the solution of Naph-Coum-COOEt in dioxane exhibited strong fluorescence upon excitation with an 820 nm laser, and the fluorescence intensified with the increasing laser power. Thus obtained good quadratic relationship between fluorescence intensity and the excitation laser power confirmed the two-photon fluorophore behavior of Naph-Coum-COOEt and the two-photon absorption (TPA) cross section was 147 GM (1 GM = 10^{-50} cm^4 s/photon). Other Coum-R and Naph-Coum-R dyes showed high TPA cross section values under 820 nm excitation (Table S1 in Supporting information). Notably, Coum-R dyes displayed larger TPA cross sections than Naph-Coum-R because the former dyes had larger molar absorptivity than the latter; the TPA cross sections of Coum-COOEt and Naph-Coum-COOEt were 292 and 147 GM, respectively.

Lipid droplets are composed of cholesterol esters and triglycerides, and the microenvironment within the LDs shows low polarity and hydrophobicity [34,35]. Because the investigated dyes exhibited distinct fluorescence properties in solvents with different polarities, we expected that our dyes would have the potential to stain LDs specifically. The cytotoxicity of Naph-Coum-COOEt and Naph-Coum-COMe was determined by MTT assays. As evident from Fig. S8, the cell viability was over 89% when cells were incubated with Naph-Coum-COOEt or Naph-Coum-COMe dyes for 24 h, indicating their low toxicity. We then chose Naph-Coum-COOEt to evaluate their staining specificity towards lipid droplets. The LD-specific dye BODIPY 493/503 was used as the reference for the co-localization experiments. As illustrated in Fig. 7, Naph-Coum-COOEt could stain LDs selectively, giving off strong red fluorescence, and its corresponding Pearson's coefficients was substantially high (0.90). Furthermore, two-photon confocal imaging experiments were performed in living cells using Naph-Coum-COOEt and Naph-Coum-COMe. As shown in Fig. 8, cells treated with these dyes exhibited strong red fluorescence sig-

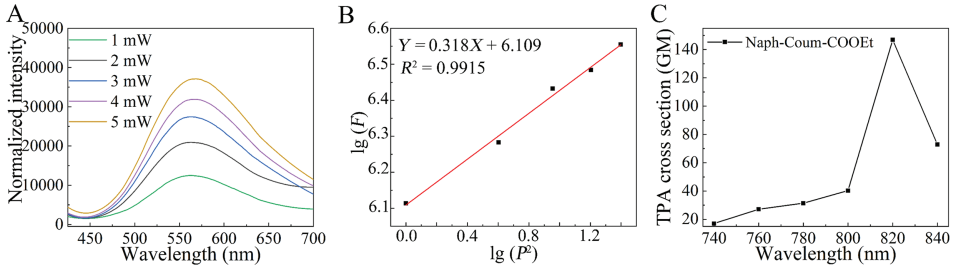

Fig. 6. (A) Wavelength-dependent TPA cross sections of Naph-Coum-COOEt in 1,4-dioxane. (B) Quadratic dependence between the fluorescence integration area and excitation laser power. (C) Two-photon excitation fluorescence spectra of Naph-Coum-COOEt in 1,4-dioxane with different laser power (λ_{ex} = 820 nm).

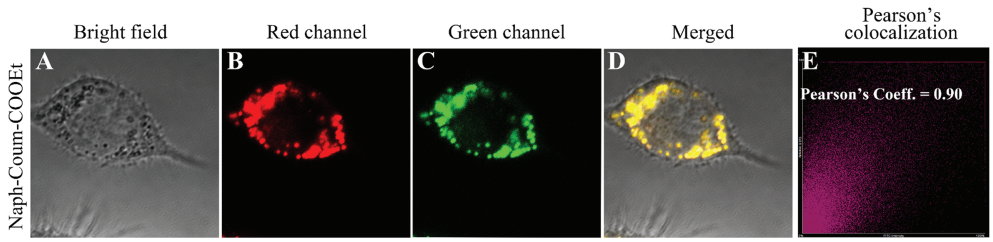

Fig. 7. (A-D) Bright filed and fluorescence images of cells incubated with Naph-Coum-COOEt (10.0 μmol/L) and BODIPY 493/503 (1.0 μg/mL) for 30 min. λ_{ex} = 405 nm. Fluorescence channels: red (570–620 nm); green (500–550 nm). Scale bar: 10 μm. (E) Pearson's colocalization coefficient of Naph-Coum-COOEt with BODIPY 493/503 as a reference.

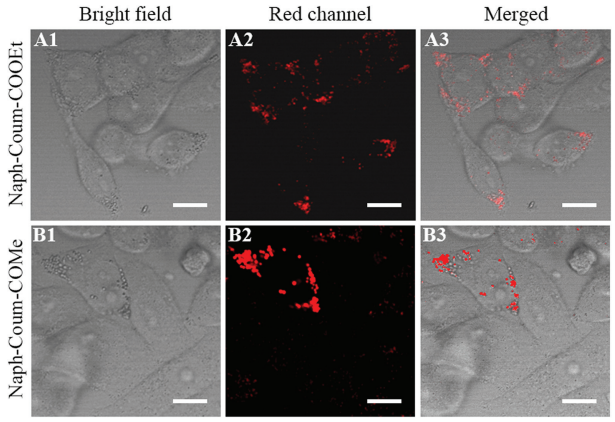

Fig. 8. Bright filed and fluorescence image of Hela cells stained with Naph-Coum-COOEt (A1-A3, top row) and Naph-Coum-COMe (B1-B3, bottom row) for 30 min, respectively. The concentration of each of the two dyes: 10.0 μmol/L). Two-photon excitation wavelength: 820 nm. λ_{em} = 570–620 nm. Scale bar: 20 μm.

nals. Thus, the imaging experiments indicated cell permeability of Naph-Coum-R dyes and thus proving their potential as LD-specific dyes for the two-photon biological imaging application.

In summary, we have rationally developed a series of coumarin-based two-photon AIE fluorophores, grouped as Naph-Coum-R and Coum-R, which displayed long-wavelength emission and large Stokes shift and high photostability. From preliminary biological experiments, these dyes could be regarded as good two-photon fluorophores capable of specifically staining LDs.

Declaration of competing interest

The authors declare that they have no known competing financial interests or personal relationships that could have appeared to influence the work reported in this paper.

Acknowledgment

This work was supported by the National Natural Science Foundation of China (No. 22178395).

Supplementary materials

Supplementary material associated with this article can be found, in the online version, at doi:10.1016/j.cclet.2022.07.017.

References

[1] C. Liu, J.L. Yin, B.L. Lu, W.Y. Lin, Sens. Actuators B: Chem. 346 (2021) 130448–130457.
[2] F. Würthner, Angew. Chem. Int. Ed. 59 (2020) 14192–14196.
[3] J. Sun, Y. Bai, Q. Ma, et al., Spectrochim. Acta A: Mol. Biomol. Spectrosc. 241 (2020) 118650–118658.
[4] Y.Z. Tu, Z. Zhao, J.W.Y. Lam, B.Z. Tang, Natl. Sci. Rev. 8 (2021) nwaa260.
[5] J.R. Zheng, S.H. Qin, L.J. Gui, et al., Chin. Chem. Lett. 32 (2021) 2385–2389.
[6] H. Turki, S. Abid, R. El Gharbi, S. Fery-Forgues, Comptes Rendus Chim. 9 (2006) 1252–1259.
[7] L. He, H.Q. Xiong, B.H. Wang, et al., Anal. Chem. 92 (2020) 11029–11034.
[8] T. Li, L.K. Wang, S.Q. Lin, et al., Bioconjug. Chem. 29 (2018) 2838–2845.
[9] K.M. Zhang, J. Shu, W.D. Chu, et al., Dye. Pigment. 185 (2021) 108898.
[10] Q.H. Hu, T. Gong, Y.Y. Mao, et al., Spectrochim. Acta A: Mol. Biomol. Spectrosc. 253 (2021) 119589.
[11] S.A. Swanson, G.M. Wallraff, J.P. Chen, et al., Chem. Mater. 15 (2003) 2305–2312.
[12] D.X. Cao, Z.Q. Liu, P. Verwilst, et al., Chem. Rev. 119 (2019) 10403–10519.
[13] E. Soini, N.J. Meltola, A.E. Soini, et al., Biochem. Soc. Trans. 28 (2000) 70–74.
[14] H.X. Fang, H. Zhang, L. Li, et al., Angew. Chem. Int. Ed. 59 (2020) 7536–7541.
[15] C.K. Jiang, L.C. Li, J.C. Jiang, et al., Chin. Chem. Lett. 31 (2020) 447–450.
[16] M.J. Jiang, R.T.K. Kwok, X.S. Li, et al., J. Mater. Chem. B 6 (2018) 2557–2565.
[17] W. Qin, P. Zhang, H. Li, et al., Chem. Sci. 9 (2018) 2705–2710.
[18] M. Jiang, X. Gu, J.W.Y. Lam, et al., Chem. Sci. 8 (2017) 5440–5446.
[19] Y.T. Gao, Y. Qu, T. Jiang, et al., J. Mater. Chem. C 2 (2014) 6353–6361.
[20] D. Kim, S. Sambasivan, H. Nam, et al., Chem. Commun. 48 (2012) 6833–6835.
[21] T. Yoshihara, R. Maruyama, S. Shiozaki, et al., Anal. Chem. 92 (2020) 4996–5003.
[22] A.R. Sarkar, C.H. Heo, H.W. Lee, et al., Anal. Chem. 86 (2014) 5638–5641.
[23] K. Sun, Y.L. Zhang, X.L. Chen, et al., ACS Appl. Bio Mater. 3 (2020) 505–511.
[24] G. Niu, R. Zhang, Y. Gu, et al., Biomaterials 208 (2019) 72–82.
[25] S.S. Ali, A. Gangopadhyay, A.K. Pramanik, et al., Dye. Pigment. 170 (2019) 107585.
[26] S. Bhalekar, S. Kothavale, N. Sekar, J. Photochem. Photobiol. A 384 (2019) 112027–112037.
[27] T.B. Ren, W. Xu, W. Zhang, et al., J. Am. Chem. Soc. 140 (2018) 7716–7722.
[28] W.B. Hu, X.F. Zhang, M.Y. Liu, J. Phys. Chem. C 125 (2021) 5233–5242.
[29] J.M. An, S.H. Kim, D. Kim, Org. Biomol. Chem. 18 (2020) 4288–4297.
[30] C. Wang, W. Chi, Q. Qiao, et al., Chem. Soc. Rev. 50 (2021) 12656–12678.
[31] J.Y. Gong, J.L. Han, Q. Liu, et al., J. Mater. Chem. C 7 (2019) 4185–4190.
[32] F. Bu, R. Duan, Y. Xie, et al., Angew. Chem. Int. Ed. 54 (2015) 14492–14497.
[33] G.L. Niu, R.Y. Zhang, J.P.C. Kwong, et al., Chem. Mater. 30 (2018) 4778–4787.
[34] G. Önal, O. Kutlu, D. Gozuacik, S. Emre, Lipids Health Dis. 16 (2017) 2–15.
[35] X. Lyu, J. Wang, J. Wang, et al., Dev. Cell. 56 (2021) 2592–2606.